Research Article

Rapid Communications in Mass Spectrometry

Received: 1 July 2014 Revised: 9 September 2014 Accepted: 19 September 2014 Published online in Wiley Online Library

Rapid Commun. Mass Spectrom. **2014**, *28*, 2690–2694
(wileyonlinelibrary.com) DOI: 10.1002/rcm.7061

Mass spectrometry studies of lycodine-type *Lycopodium* alkaloids: sauroxine and *N*-demethylsauroxine

Diego A. Cifuente[1]*, Mariana G. Vallejo[2], Maria G. Ortega[2], José L. Cabrera[2], Víctor S. Martín[3], Carlos E. Tonn[1], Alicia M. Agnese[2] and Carlos E. Ardanaz[1]*

[1]INTEQUI-CONICET, Área de Química Orgánica, Facultad de Química, Bioquímica y Farmacia, Universidad Nacional de San Luis, Chacabuco y Pedernera, 5700 San Luis, Argentina
[2]IMBIV-CONICET, Farmacognosia, Departamento de Farmacia, Facultad de Ciencias Químicas, Universidad Nacional de Córdoba, 5000 Córdoba, Argentina
[3]Instituto Universitario de Bio-Orgánica 'Antonio González', Universidad de La Laguna, Avda. Astrofísico Francisco Sánchez,' 2, La Laguna 38206,' Tenerife, Spain

RATIONALE: Sauroxine and *N*-demethylsauroxine are lycodine-type *Lycopodium* alkaloids. In recent years, *Lycopodium* alkaloids have gained significant interest due to their unique skeletal characteristics as well as due to their acetylcholinesterase activity. It is known that drugs that inhibit acetylcholinesterase can be used to treat the early stages of Alzheimer's disease.
METHODS: Sauroxine and *N*-demethylsauroxine were isolated from the aerial parts of *Huperzia saururus* (Lam.) Trevis. Electron ionization mass spectrometry (EI-MS) (low resolution) and collision-induced dissociation tandem mass spectrometry (CID-MS/MS) fragmentation was conducted using an ion trap, GCQ Plus mass spectrometer with MS/MS. Electron ionization high-resolution mass spectrometry (EI-HRMS) was performed in a magnetic sector mass spectrometer (Micromass VG).
RESULTS: Using GC/EI-CID-MS/MS we obtained different fragmentation routes that connect all the ionic populations. In addition, the use of EI-HRMS allowed us to measure the exact masses of all the fragment ions, and, with all this information gathered, we tried to establish a fragmentation scheme concordant with the ascendant and descendant species.
CONCLUSIONS: The mass spectrometry studies presented in this work complete our mass studies of *Lycopodium* alkaloids. The mass spectrometry work presented has been very useful to confirm the structures as well as to support the biogenetic relationships between the lycodine-type *Lycopodium* alkaloids: sauroxine and *N*-demethylsauroxine.

The *Lycopodium* alkaloids are a family of structurally diverse and bioactive natural products.[1] In recent years, these alkaloids have attracted significant interest due to their unique skeletal characteristics as well as because of their biological activities.[2,3] Taking into account the structural characteristics and biogenetic relationships, the *Lycopodium* alkaloids can be divided into four different structural classes: the lycodine class (Fig. 1(a)), the lycopodine class (Fig. 1(b)), the fawcettimine class (Fig. 1(c)) and the miscellaneous class (Fig. 1(d)).

On the other hand, the most significant bioactivity that has been elucidated in *Lycopodium* alkaloids is selective and reversible acetylcholinesterase inhibition and/or effects on memory-related phenomena.[4] The inhibition of acetylcholinesterase has been shown to improve symptoms in patients with Alzheimer's disease (AD).[5] It is known that AD, a neurodegenerative disease of significant socioeconomic impact, is associated with deficits in brain neurotransmitters, especially acetylcholine. In this respect, the discovery of new *Lycopodium* alkaloids possessing an activity on learning and on memory seems to be promising in the treatment of AD.

In previous studies, we isolated from *Huperzia saururus* (Lam.) Trevis. ('cola de quirquincho', Lycopodiaceae) *Lycopodium* alkaloids[6] and we reported the bioactivity of the major alkaloids: sauroine and sauroxine (**1**) (Fig. 2). Sauroine, a *Lycopodium* alkaloid of the lycopodine-type, strongly enhances hippocampal long term potentiation (LTP) as well as memory retention, demonstrated in *vivo*.[7] At the same time, it was not an inhibitor of the acetylcholinesterase enzyme. On the contrary, compound **1**, a *Lycopodium* alkaloid of the lycodine-type, was an acetylcholinesterase inhibitor, but had no effect on LTP.[7]

On the other hand, we had previously reported the mass spectrometric study of sauroine.[8] In this work, we focus on the application of mass spectrometry to support the structural determination of the lycodine-type *Lycopodium* alkaloids:

* *Correspondence to:* D. A. Cifuente and C. E. Ardanaz, Área de Química Orgánica, Facultad de Química, Bioquímica y Farmacia, Universidad Nacional de San Luis, Chacabuco y Pedernera, 5700 San Luis, Argentina.
E-mail: diegocifuente@gmail.com; ardanaz@unsl.edu.ar

Rapid Communications in Mass Spectrometry

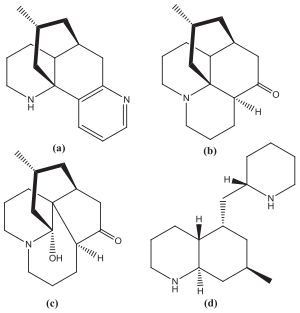

Figure 1. *Lycopodium* alkaloids: lycodine class (a), lycopodine class (b), fawcettimine class (c) and miscellaneous class (d).

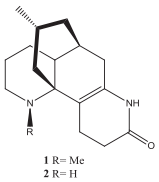

Figure 2. Structure of sauroxine (1) and *N*-demethylsauroxine (2).

Table 1. Accurate mass measurements and elemental formulae of the main abundant ionic species of compound 1 obtained by GC/EI-HRMS

Mass	Calc. Mass	ppm	Formula
274,2050	274,2045	1.8	$C_{17}H_{26}N_2O$
232,1692	232,1701	−3.9	$C_{15}H_{22}NO$
232,1563	232,1576	−5.6	$C_{14}H_{20}N_2O$
231,1633	231,1623	4.3	$C_{15}H_{21}NO$
231,1505	231,1497	3.5	$C_{14}H_{19}N_2O$
218,1408	218,1419	−5	$C_{13}H_{18}N_2O$
217,1457	217,1467	−4.6	$C_{14}H_{19}NO$
217,1337	217,1341	−1.8	$C_{13}H_{17}N_2O$
203,1296	203,1310	−6.9	$C_{13}H_{17}NO$
203,1165	203,1184	−9.4	$C_{12}H_{15}N_2O$
189,1146	189,1154	−4.2	$C_{12}H_{15}NO$
189,1024	189,1028	−2.1	$C_{11}H_{13}N_2O$
175,1007	175,0997	5.7	$C_{11}H_{13}NO$

sauroxine (**1**) and *N*-demethylsauroxine (**2**)[9] (Fig. 2). We describe and discuss the electron ionization mass spectrometry (GC/EI-MS) (low resolution, LR) data recorded with a QIT-MS instrument and collision-induced dissociation tandem mass spectrometry fragmentation (CID-MS/MS) for alkaloids **1** and **2**.

EXPERIMENTAL

Compounds **1** and **2** were previously isolated from the aerial parts of *Huperzia saururus* (Lam.) Trevis.[6,9] The EI-HRMS measurements were obtained from a Micromass VG AutoSpec (Manchester, UK), at the Instituto Universitario de Bioorgánica (Universidad de La Laguna), at a resolution of 5000 (5% valley definition), by 70 eV electron ionization, at an accelerating voltage of 8 kV. EI-LRMS was performed using an ion trap, GCQ Plus, with MS/MS (Finnigan, Thermo-Quest, Austin, TX, USA), operated at fundamental rf-drive of 1.03 MHz. EI spectra were obtained at an average electron energy of 70 eV. Helium was used as the damping gas at an uncorrected gauge reading of 6×10^{-5} Torr. For the analysis of (CID) product ions, the precursor was selected using a MS/MS standard function, with 0.5–1.0 Da peak width for the precursor ion, and dynamically programmed scans. The supplementary voltage was in the range 0.5–1.0 V, as described previously.[10,11]

RESULTS AND DISCUSSION

Compounds **1** and **2** exhibited molecular ions at *m/z* 274 and *m/z* 260 corresponding to the molecular formulas $C_{17}H_{26}N_2O$ and $C_{16}H_{24}N_2O$, respectively.[6,9] In addition, the use of EI-HRMS enables us to describe in detail the fragmentation pathways. Tables 1–4 present the proposed elemental compositions of the main fragments obtained by EI-HRMS and the identities of the major ions, obtained by gas chromatography (GC)/EI-CIDMS/MS for **1** and **2**, respectively. The general proposed fragmentation patterns of **1** and **2**, obtained by GC/EI-CID-MS/MS, are depicted in Schemes 1–3.

Table 2. Collision spectra of the main abundant ionic species of compound **1** obtained by GC/EI-CID-MS/MS

Precursor ions selected by EI-MS	**Product ions (scan used MS^2)**					
m/z (%)	*m/z* (%)	*m/z* (%)	*m/z* (%)	*m/z* (%)	*m/z* (%)	*m/z* (%)
231 (56.1)	216 (5.4)	215 (4.7)	203 (7.8)	201 (8.7)	189 (100.0)	174 (12.6)
	172 (8.4)	161 (26.4)	160 (26.6)	146 15.3)	134 (8.9)	
218 (3.1)	203 (69.6)	202 (7.3)	190 (100.0)	189 (18.1)	175 (6.8)	164 (6.7)
	162 (3.2)	161 (3.0)	162 (3.2)	161 (3.0)		
217 (3.1)	202 (2.7)	189 (100.0)	175 (3.1)	174 (3.0)	161 (0.7)	148 (1.0)
	147 (1.3)					
203 (41.2)	201 (6.2)	188 (21.9)	186 (26.7)	185 (10.4)	175 (19.5)	161 (100.0)
	159 (30.6)	148 (38.4)	147 (54.7)	146 (18.3)	132 (23.9)	159 (30.6)
189 (31.7)	174 (100.0)	146 (46.3)	145 (13.3)	133 (8.3)	132 (9.0)	119 (13.4)
	118 (11.5)	106 (10.3)	118 (11.5)	106 (10.3)	118 (11.5)	106 (10.3)

Table 3. Accurate mass measurements and elemental formulae of the main abundant ionic species of compound **2** obtained by GC/EI-HRMS

Mass	Calc. mass	ppm	Formula
260,1896	260,1889	2.7	$C_{16}H_{24}N_2O$
218,1428	218,1419	4.1	$C_{13}H_{18}N_2O$
217,1357	217,1341	7.4	$C_{13}H_{17}N_2O$
203,1183	203,1184	−0.5	$C_{12}H_{15}N_2O$
189,1163	189,1154	4.8	$C_{12}H_{15}NO$
189,1041	189,1028	6.9	$C_{11}H_{13}N_2O$
175,0878	175,0871	4	$C_{10}H_{11}N_2O$

Using GC/EI-CID-MS/MS, we obtained the different fragmentation routes that connect all the ionic populations. The use of GC/EI-HRMS allowed us to measure the exact masses of all the fragment ions, and, with all this data gathered, we tried to establish a fragmentation scheme concordant with the ascendant and descendant species.

In Scheme 1, the CID-MS/MS fragmentation of the molecular ion of **1** ($M^{+\cdot}$ *m/z* 274) afforded the fragments: $[C_{15}H_{21}NO]^+$ at *m/z* 231 by the loss of *N*-methylenemethanamine ($-C_2H_5N$, −43 Da) and $[C_{11}H_{12}NO]^{\cdot\,+}$ at *m/z* 174 *via* the elimination of the isobutyl bridge ($-C_4H_9$, −57 Da) (route a). Also, in the CID-fragmentation route b, the precursor radical

Table 4. Collision spectra of the main abundant ionic species of compound **2** obtained by GC/EI-CID-MS/MS

Precursor ions selected by EI-MS	**Product ions (scan used MS^2)**					
m/z (%)	*m/z* (%)	*m/z* (%)	*m/z* (%)	*m/z* (%)	*m/z* (%)	*m/z* (%)
217 (89.6)	203 (55.2) 144 (31.2)	201 (24.0) 133 (27.1)	189 (42.7)	175 (100.0)	174 (30.2)	161 (22.9)
203 (7.0)	202 (0.7) 147 (3.2)	188 (1.2) 133 (0.9)	175 (100.0)	161 (1.8)	160 (1.5)	157 (5.3)
189 (20.5)	174 (22.2) 132 (10.9)	171 (11.6) 108 (15.4)	154 (18.4)	147 (100.0)	135 (12.5)	133 (20.8)

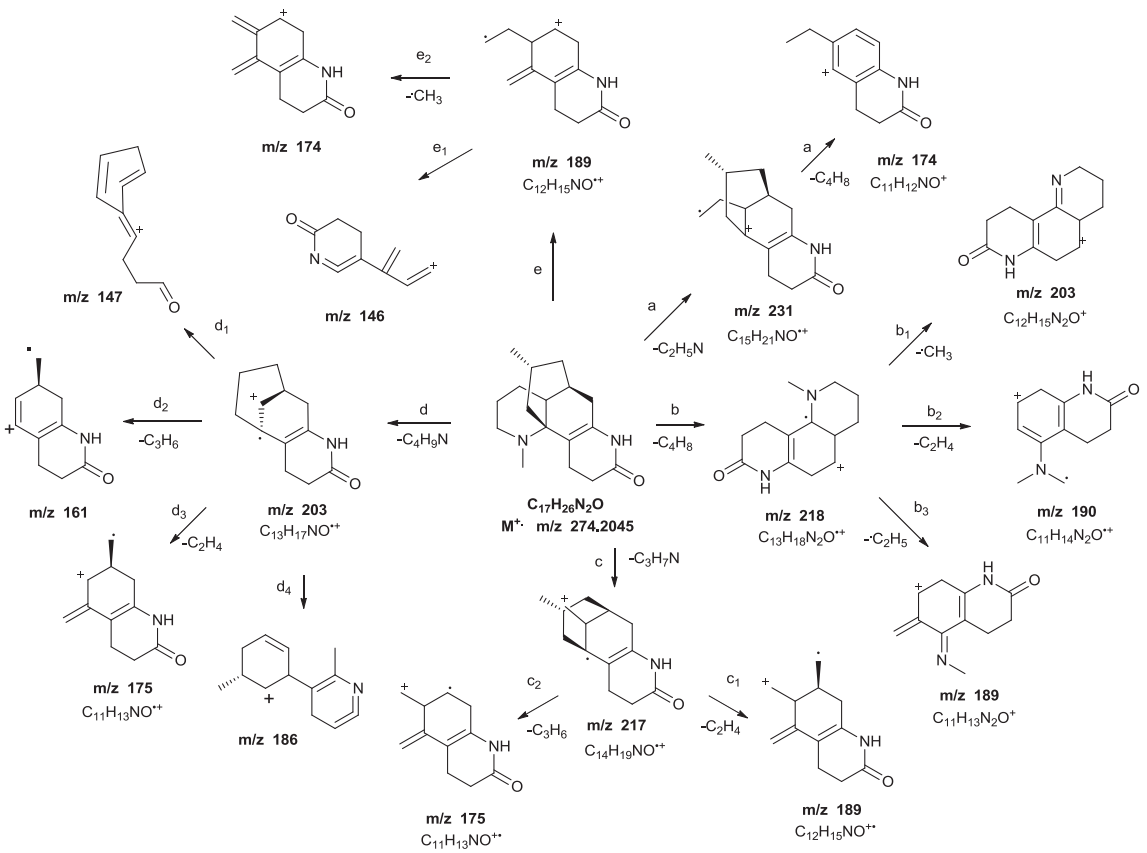

Scheme 1. Molecular ion fragmentation pattern by GC/EI-MS/MS of **1**.

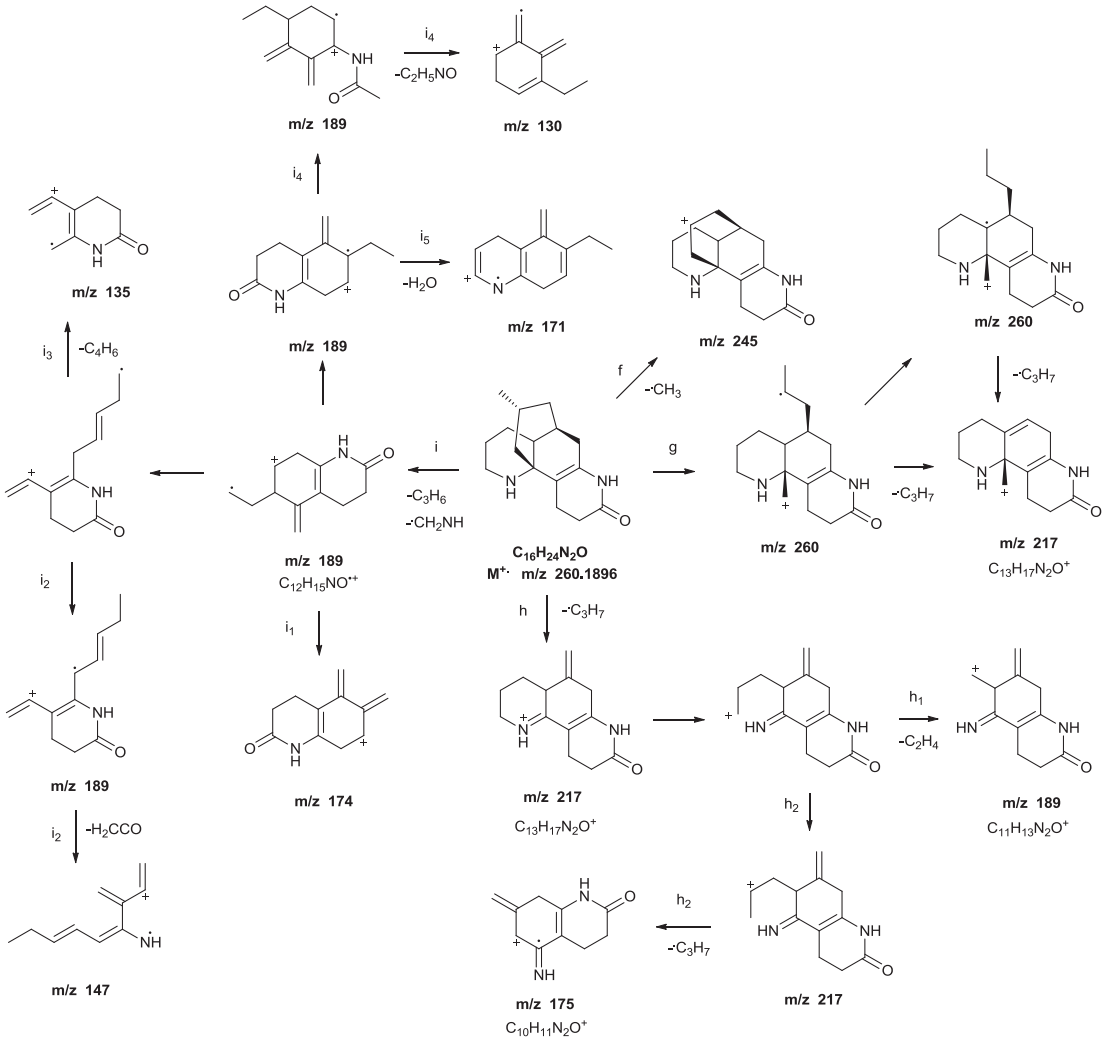

Scheme 2. Molecular ion fragmentation pattern by GC/EI-MS/MS of **2**.

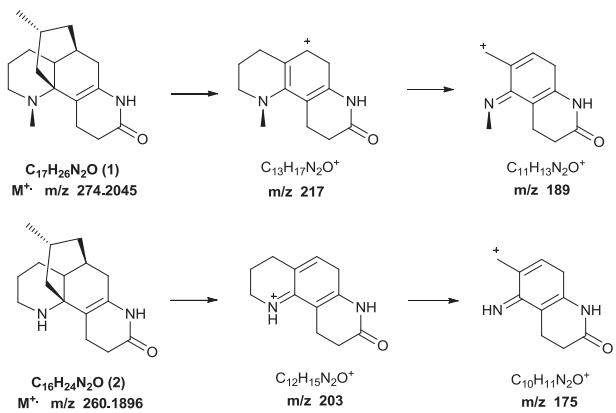

Scheme 3. Molecular ion fragmentation pattern by GC/EI-MS/MS of **1** and **2**.

ion can lose an isobutylene group ($-C_4H_8$, −56 Da) to produce the radical cation $[C_{13}H_{18}N_2O]^{\cdot+}$ at *m/z* 218. Sequentially, the latter fragment can eliminate a methyl radical ($-CH_3$, −15 Da), an ethylene molecule ($-C_2H_4$, −28 Da) or an ethyl radical ($-C_2H_5$, −29 Da), to form the ions $[C_{12}H_{15}N_2O]^+$ at *m/z* 203, $[C_{11}H_{14}N_2O]^{\cdot+}$ at *m/z* 190 and $[C_{11}H_{13}N_2O]^{\cdot+}$ at *m/z* 189, respectively (Scheme 1, routes b_1–b_3). In the same scheme, route c involves the elimination of C_3H_7N (−57 Da) to yield the ion $[C_{14}H_{19}NO]^{\cdot+}$ at *m/z* 217. This fragment gave the radical cations $[C_{11}H_{13}NO]^{\cdot+}$ at *m/z* 175 and $[C_{12}H_{15}NO]^{\cdot+}$ at *m/z* 189 *via* removal of propylene and ethylene molecules, C_3H_6 (−42 Da) and C_2H_4 (−28 Da), respectively (routes c_1 and c_2). Alternatively, the precursor ion at *m/z* 274,can lose C_4H_9N (−71 Da) to afford the fragment $[C_{13}H_{17}NO]^{\cdot+}$ at *m/z* 203 (route d). Then, in routes d_1–d_4, the latter fragment produces the following four ions: *m/z* 147, *m/z* 161, involving the loss of a molecule of propene ($-C_3H_6$, −42 Da), $[C_{11}H_{13}NO]^{\cdot+}$ at *m/z* 175 *via* elimination of

ethylene ($-C_2H_4$, −28 Da) and the fragment *m/z* 186. Finally, in route e (Scheme 1), the molecular precursor at *m/z* 274 is fragmented to form the radical cation $[C_{12}H_{15}NO]^{\cdot+}$ at *m/z* 189. This fragment undergoes further rearrangements and affords the ions at *m/z* 174 and *m/z* 146, respectively (Scheme 1, routes e_1 and e_2).

In Scheme 2, the CID-MS/MS of the molecular radical ion of **2** at *m/z* 260 afforded the product ion at *m/z* 245 by elimination of a methyl radical (route f). Rearrangement of the precursor radical ion at *m/z* 260, followed by the loss of the propyl radical ($-C_3H_7$, −43 Da) afforded the product ion $[C_{13}H_{17}N_2O]^+$ at *m/z* 217 (route g). Alternatively, the precursor radical ion may lose a propyl radical ($-C_3H_7$, −43 Da), in another position, to give the product ion $[C_{13}H_{17}N_2O]^+$ at *m/z* 217 (Scheme 2, route h). This latter product ion can further rearrange by losing a molecule of ethylene ($-C_2H_4$, −28 Da) to form the secondary product ion $[C_{11}H_{13}N_2O]^+$ at *m/z* 189 (route h_1). The product ion at *m/z* 217 fragments via route h_2 (Scheme 2) by a concomitant rearrangement and elimination of the *n*-propyl radical ($-C_3H_7$, −43 Da) to form the secondary product ion $[C_{10}H_{11}N_2O]^+$ at *m/z* 175. Alternatively, the precursor ion at *m/z* 260 can lose a molecule of propene ($-C_3H_6$, −42 Da) and the -CH_2NH group (−29 Da) to form the radical cation $[C_{12}H_{15}NO]^{+\cdot}$ at *m/z* 189 (Scheme 2, route i). Sequentially in route i_1, the product radical ion at *m/z* 189 produces the product ion at *m/z* 174 by loss of a methyl radical. Route i_2 involves the fragmentation of *m/z* 189 via consecutive rearrangement involving the loss of a molecule of ketene (−42 Da), ethenone, to afford the ion at *m/z* 147. Similarly, the ion at *m/z* 189 can fragment via consecutive rearrangement followed by loss of a butadiene molecule ($-C_4H_6$, −54 Da) to afford the radical cation at *m/z* 135 (Scheme 2, route i_3). Finally, the fragment $[C_{12}H_{15}NO]^{+\cdot}$ yields the radical cations at *m/z* 130 and *m/z* 171, through further rearrangements and elimination of ethanamide ($-C_2H_5NO$, −47 Da) and water, respectively (Scheme 2, routes i_4 and i_5).

In Scheme 3, the fragmentations of alkaloids **1** and **2** show a similar behavior, involving the loss of the isobutyl bridge followed by ethylene to produce the ions: $[C_{13}H_{17}N_2O]^+$ at *m/z* 217 and $[C_{12}H_{13}N_2O]^+$ at *m/z* 189, in the CID-MS/MS of sauroxine (**1**) or the ions $[C_{12}H_{15}N_2O]^+$ at *m/z* 203 and $[C_{10}H_{11}N_2O]^+$ at *m/z* 175 in the mass spectrum of *N*-demethylsauroxine (**2**).

In conclusion, the mass spectrometry studies presented in this paper have been very useful to confirm the structures as well as to support the biogenetic relationships between lycodine-type *Lycopodium* alkaloids sauroxine (**1**) and *N*-demethylsauroxine (**2**).

Acknowledgements

This work has been financially supported by CONICET (PIP 2010/2012-00607 and 2009/2011-00628), UNSL (Project 22/Q805), ANPCyT (PICT-2007-352 and PICT 2010–1576), UNC (Project 05/C548), ME (PPUA-Res 288SPU/2011), SeCyT-UNC (Res 214/10), Spanish MEC co-financed by the European Regional Development Fund (CTQ2008-06806-C02-01/BQU) and Canary Islands ACIISI (PI 2007/021) co-financed by the European FEDER. Also, we thank Dr. Sergio Suárez Izquierdo (IUBO, Universidad de La Laguna) for the HRMS measurements.

REFERENCES

[1] X. Ma, D. R. Gang. The *Lycopodium* alkaloids. *Nat. Prod. Rep.* **2004**, *21*, 752.
[2] Y. Hirasawa, J. I. Kobayashi, H. Morita. The *Lycopodium* alkaloids. *Heterocycles* **2009**, *77*, 679.
[3] X. Ma, C. Tan, D. Zhu, D. R. Gang, P. Xiao. Huperzine A from *Huperzia* species – An ethnopharmacological review. *J. Ethnopharmacol.* **2007**, *113*, 15.
[4] E. Steinunn Halldorsdottir, J. W. Jaroszewski, E. S. Olafsdottir. Acetylcholinesterase inhibitory activity of lycopodane-type alkaloids from the Icelandic *Lycopodium annotinum* ssp. *alpestre*. *Phytochemistry* **2010**, *71*, 149.
[5] M. Mehta, A. Adem, M. Sabbagh. New acetylcholinesterase inhibitors for Alzheimer's disease. *Int. J. Alzheimer Dis.* **2012**, *1*, 1.
[6] M. G. Ortega, A. M. Agnese, J. L. Cabrera. Sauroine – a novel *Lycopodium* alkaloid from *Huperzia saururus*. *Tetrahedron Lett.* **2004**, *45*, 7003.
[7] M. G. Vallejo, S. Loyola, D. Contreras, G. Ugarte, D. A. Cifuente, M. G. Ortega, J. L. Cabrera, M. Zeise, C. E. Tonn, M. Carreño, R. Delgado, B. Morales, A. M. Agnese. A new semisynthetic derivative of sauroine induces LTP hippocampal slices and improves learning performance in the Morris Water Maze. *J. Neurochem.* **2014**, *129*, 864.
[8] M. G. Vallejo, D. A. Cifuente, F. M. Cecati, M. G. Ortega, J. L. Cabrera, V. S. Martín, C. E. Tonn, A. M. Agnese, C. E. Ardanaz. Mass spectrometry studies of *Lycopodium* alkaloid sauroine. *Rapid Commun. Mass Spectrom.* **2012**, *26*, 2827.
[9] M. G. Vallejo, M. G. Ortega, J. L. Cabrera, A. M. Agnese. *N*-Demethylsauroxine, a novel Lycodine group alkaloid from *Huperzia saururus*. *Tetrahedron Lett.* **2013**, *54*, 5197.
[10] C. R. Pungitore, C. García, V. S. Martín, C. E. Tonn, C. E. Ardanaz. Mass spectrometry studies of iridoid aglycone derivatives. *Rapid Commun. Mass Spectrom.* **2011**, *25*, 2099.
[11] G. F. Reta, F. M. Cecati1, N. A. Teruel, P. C. Rossomando, O. J. Donadel, V. S. Martín, C. E. Tonn, M. Kurina-Sanz, C. E. Ardanaz. Mass spectral studies of diamide compounds obtained by the Ugi reaction. *Rapid Commun. Mass Spectrom.* **2013**, *27*, 2033.

